HEDL-TME 73-30
ENDF-171
UC-79d

NEUTRON RESONANCE SPACINGS FOR SPHERICAL NUCLEI

F. SCHMITTROTH

JANUARY 1973

HANFORD ENGINEERING DEVELOPMENT LABORATORY **P.O. Box 1970 Richland, WA 99352**
Operated by Westinghouse Hanford Company
A Subsidiary of Westinghouse Electric Corporation

Prepared for the U.S. Atomic Energy Commission
Division of Reactor Development and Technology
under Contract No. AT(45-1)-2170

NEUTRON RESONANCE SPACINGS

FOR SPHERICAL NUCLEI

F. Schmittroth

ABSTRACT

Theoretical single-particle level densities are computed for a Woods-Saxon potential to estimate average neutron-resonance spacings for spherical nuclei. This average spacing D_{obs} is a key parameter for neutron-capture calculations. Experimental values for D_{obs}, which are evaluated for about 85 nuclei using recent data, are used to improve the theoretical estimates. Special care is given to the identification of p-wave resonance in these evaluations.

TABLE OF CONTENTS

ILLUSTRATIONS

TABLES

I. INTRODUCTION

In order to compute average neutron-capture cross sections, one must know the average spacing between the resonances seen in low energy neutron scattering[1]. In fact, these cross sections are roughly inversely proportional to the average neutron-resonance spacing, so that any uncertainty in this spacing is directly reflected in the computed cross sections. At low energies, most of the resonances are due to s-wave neutrons, and we denote the average spacing observed between s-wave resonances by D_{obs}. Unfortunately, for many fission-product isotopes where theoretical capture cross sections are needed, too few neutron resonances have been measured to give reliable estimates of D_{obs}. If experimental neutron-capture data are available in these cases, D_{obs} may be treated as an adjustable parameter. Otherwise, it is necessary to have some other way to estimate D_{obs}.

There is a long history of theoretical attempts to predict the average resonance spacing D_{obs}[2-7]. This spacing represents a direct measurement of the density of levels in the compound nucleus at the neutron binding energy and plays a fundamental role in nuclear physics. In addition, there have been phenomenological studies[4,7] of D_{obs} motivated by the requirements of neutron-capture calculations. In spite of this effort, there are large discrepancies in the predicted values of D_{obs} given by various workers for many isotopes. This is not surprising when one notes that values from D_{obs} vary from a few eV to many keV. However, even in the cases where D_{obs} was determined experimentally, there may be large discrepancies among the reported values due to poor data or to differing evaluation procedures.

In this work we have used recent theoretical developments to give improved estimates of D_{obs}. In particular, Strutinsky averaging[8,9] applied to a Woods-Saxon shell-model potential was used to calculate the average single-particle level densities. At the same time we have made a literature search for experimental data[10-22] in order to obtain the best possible experimental values for D_{obs}. These values were used to test the theoretical results and to provide phenomenological adjustments to the theoretical predictions.

We have limited this study to spherical nuclei between copper (Z = 29) and samarium (Z = 62) to reduce the work that a more comprehensive study would entail and to avoid the theoretical problems associated with deformed nuclei[8,9]. This region is important for our own neutron capture work.

II. THEORETICAL ESTIMATES OF D_{obs}

A. Level Density Formalism

In this section we present the theoretical basis for our analysis. The problem is to compute the density of levels in the compound nucleus at an excitation energy equal to the binding energy of the last neutron. Nearly all recent theoretical work begins with the independent-particle model of the nucleus with corrections made for residual interactions[23]. Statistical mechanics can then be used to relate the density of levels in the compound nucleus to the density of states for the individual neutrons and protons (see for example the work of Gilbert and Cameron[3] whose formalism we follow here).

The density of levels in the compound nucleus $\rho(E)$ is related to the

single-particle states by

$$\rho(E) = \frac{1}{(2\pi)^2\sqrt{D(\Omega)}} \exp\,(\Omega-\alpha_N N-\alpha_Z Z-\alpha_M M+\beta E), \qquad (1)$$

where N, Z, M, and E are the total number of neutrons, the total number of protons, the magnetic quantum number, and the energy, respectively. The temperature is $t = 1/\beta$, while the α_i's are appropriate chemical potentials. The denominator $D(\Omega)$ is a Jacobian of Ω. The detailed single-particle properties are found in Ω, which for the independent-particle model of the nucleus, is given by

$$\Omega = \Omega_N + \Omega_Z,$$

and

$$\Omega_N = \sum_i \log\left[1 + \exp\,(\alpha_N+\alpha_3 m_{Ni}-\beta\varepsilon_{Ni})\right], \qquad (2)$$

with a similar expression for Ω_Z. The i-sum is over all single-particle neutron states. The neutron energies and magnetic quantum numbers are denoted by ε_{Ni} and m_{Ni} respectively.

In order to arrive at a simple expression for the level density, the i-sum in Eq. (2) is replaced by an integral over the single particle level density:

$$\sum_i \log\left[1 + \exp\,(\alpha_N+\alpha_3 m_{Ni}-\beta\varepsilon_{Ni})\right]$$

$$\cong \sum_{m_N} \int d\varepsilon \left\{ g_N(\varepsilon,m_N) \log\left[1 + \exp\,(\alpha_N+\alpha_3 m_N-\beta\varepsilon)\right]\right\}, \qquad (3)$$

where $g_N(\varepsilon, m_N)$ is the density of neutron states with energy ε and magnetic quantum number m_N. This "continuous approximation" breaks down for very low excitation energies[24]. Rosenzeig[25] has shown there may be errors introduced by this approximation even at the higher energies that interest us. These effects have never been conclusively observed, however, and we do not consider them further.

After a considerable amount of algebra and a few less significant approximations, one finds the following expression for the density of levels at energy E with spin J:

$$\rho(E,J) = \frac{(2J+1)}{24\sqrt{2}\,\sigma^3\, a^{1/4}\, U^{5/4}} \exp\left[-\frac{(J+\frac{1}{2})^2}{2\sigma^2}\right] \exp\left(2\sqrt{aU}\right). \qquad (4)$$

This density includes both parities but does <u>not</u> include the (2J+1) m-degeneracy. The effective excitation energy is $U = E - P$ where P is a phenomenological value for the pairing. A more fundamental approach[26] is to introduce the pairing interaction directly into Eq. (2). However, the resulting equations are very complicated. The single-particle level densities for neutrons and protons are combined into the single parameter <u>a</u>:

$$a = a_N + a_Z \,,$$

$$a_N = \frac{\pi^2}{6} g_N \,, \qquad (5)$$

$$a_Z = \frac{\pi^2}{6} g_Z \,,$$

where g_N and g_Z are the total single-particle densities for neutrons and protons, respectively

$$g_N(\varepsilon) = \sum_{m_N} g_N(\varepsilon, m_N) \quad ,$$

$$g_Z(\varepsilon) = \sum_{m_Z} g_Z(\varepsilon, m_Z) \quad , \tag{6}$$

$$g = g_N + g_Z \quad .$$

The spin-cutoff parameter σ is given by

$$\sigma^2 = g \langle m^2 \rangle t \quad , \tag{7}$$

where the nuclear temperature is found from

$$t = 1/\beta \cong \sqrt{U/a} \quad . \tag{8}$$

The average square magnetic quantum number is defined by

$$\langle m^2 \rangle g(\varepsilon) = \sum_{m_N} m_N^2 g_N(\varepsilon, m_N) + \sum_{m_Z} m_Z^2 g_Z(\varepsilon, m_Z) \quad . \tag{9}$$

Since s-wave neutrons excite only compound nucleus states with a single parity and with spin $J = I \pm 1/2$ where I is a nonzero target spin, the observed s-wave spacing of neutron resonances D_{obs} is related to the density $\rho(E,J)$ by

$$1/D_{obs} = \frac{1}{2} \sum_{J=I-\frac{1}{2}}^{J=I+\frac{1}{2}} \rho(B_n, J) \quad . \tag{10}$$

For $I = 0$, the only term in the sum is $J = \frac{1}{2}$. B_n is the neutron binding energy. This last equation completes the connection between observed neutron-resonance spacings and single-particle level densities.

With the above formulas, the level density $\rho(E)$ can be computed once the level density parameter a is known. From Eq. (3), it is seen that the average single-particle densities g_N and g_Z should represent averages over an energy region of about $1/\beta$. Strutinsky[8] has given a simple prescription for averaging shell-model level densities. Although he used his method to find shell-model corrections to liquid-drop energies, it is nonetheless suitable for our purposes.

B. Strutinsky-Averaged Shell-Model Densities

In this section we show how to find g_N and g_Z from single-particle states generated by a Woods-Saxon potential. The neutrons and protons are treated independently throughout so that it is convenient to define a subscript s to represent neutrons (s = N) or protons (s = Z).

Given a set of neutron and proton single-particle energies (ε_{1s}, ε_{2s}, ...), Strutinsky's prescription is to use a Gaussian weighting function to compute the average level densities

$$g_s(\varepsilon_{fs}) = \frac{1}{\sqrt{\pi}\,\gamma} \sum_i \exp\left[-\frac{(\varepsilon_{fs}-\varepsilon_{is})^2}{\gamma^2}\right] \qquad (11)$$

where $\{\varepsilon_{fs},\ s = N,Z\}$ are the neutron and proton Fermi energies, and γ defines the weighting interval. As expressed here, the i-sum must include any single-particle degeneracies.

The actual number of neutrons or protons which correspond to a given Fermi energy is found from

$$N_s(\varepsilon_{fs}) = \int_0^{\varepsilon_{fs}} g_s(\varepsilon)\, d\varepsilon \quad . \qquad (12)$$

A rather annoying systematic dependence of these densities on the total atomic mass may be removed by defining a mass independent energy $\bar{\varepsilon}$:

$$\varepsilon = \hbar\omega\, \bar{\varepsilon} \quad , \qquad (13)$$

where the mass dependence is given by the factor $\hbar\omega = 41 / A^{1/3}$ With this change of variable, Eqs. (11) and (12) become

$$\bar{g}_s\ (\bar{\varepsilon}_{fs}) = \frac{1}{\sqrt{\pi}\ \bar{\gamma}} \sum_i \exp\left[- \frac{(\bar{\varepsilon}_{fs} - \bar{\varepsilon}_{is})^2}{\bar{\gamma}^2} \right] , \qquad (14)$$

and

$$N_s\ (\bar{\varepsilon}_{fs}) = \int_0^{\bar{\varepsilon}_{fs}} \bar{g}_s(\bar{\varepsilon})\ d\bar{\varepsilon} \quad , \qquad (15)$$

where

$$\bar{\varepsilon} = \varepsilon\ /\ \hbar\omega \quad , \qquad (16a)$$

for all energies, and

$$\bar{\gamma} = \gamma\ /\ \hbar\omega \quad , \qquad (16b)$$

$$\bar{g}_s = \hbar\omega\ g_s \quad . \qquad (16c)$$

C. Calculation of Single-Particle Energies

Since we have restricted our work to the mass region where nuclei are spherical, we use a Woods-Saxon potential to calculate the single-particle energy eigenvalues $\{ \varepsilon_{is} \}$. That is, we find solutions to the single-particle Schroedinger equation

$$(T + V)\ \phi_{is} = \varepsilon_{is}\ \phi_{is} \quad , \tag{17}$$

where the ϕ_{is} are the eigenfunctions for a particle bound in a potential well V(r) with kinetic energy T. (Recall that s = N,Z for neutrons, protons.)

The potential energy for neutrons is given by[27]

$$V(r) = V_o\ f(r) + V_{so}\ \bar{l}.\bar{s}\ r_0^2\ \frac{1}{r}\ \frac{df}{dr} \tag{18a}$$

where

$$f(r) = [1 + \exp\ (\frac{r-R}{a})]^{-1} \tag{18b}$$

with

$$V_o = -51 + 33\ (\frac{N-Z}{A}) \quad , \tag{18c}$$

$$V_{so} = -0.44\ V_o \quad , \tag{18d}$$

$$R = r_o\ A^{1/3}, \quad r_o = 1.27 \tag{18e}$$

and

$$a = 0.67 \quad . \tag{18f}$$

For protons, a coulomb potential is added and V_o becomes

$$V_o = -51 - 33 \left(\frac{N-Z}{A}\right) \quad . \tag{19}$$

All energy units are in MeV, and lengths are in Fermis.

Figure 1 shows the single-particle energies ε_{is} in units of $\hbar\omega$ for both neutrons and protons. The mass number A used to calculate each difference was determined as follows: The number of neutrons or protons, as the case may be, was taken to be the average of the occupation numbers for the two successive levels. The line of beta stability was then used to relate the mass number A to the number of neutrons or protons.

The above equations were used to find $\bar{g}_s(\bar{\varepsilon}_{fs})$ and $N_s(\bar{\varepsilon}_{fs})$. The occupation numbers $N_s(\bar{\varepsilon}_{fs})$, shown in Figure 2 for neutrons, were then used to obtain the level densities $\bar{g}_s$ as a function of the occupation numbers N_g. These results, displayed in Figure 3, are expressed in terms of the level density parameters $\underline{a}_s$ and show how the single-particle level densities vary with the number of neutrons or protons.

The averaging width γ should be typical of the temperature $t = 1/\beta$ which appears in Eq. (3). The excitation energies of the compound nucleus

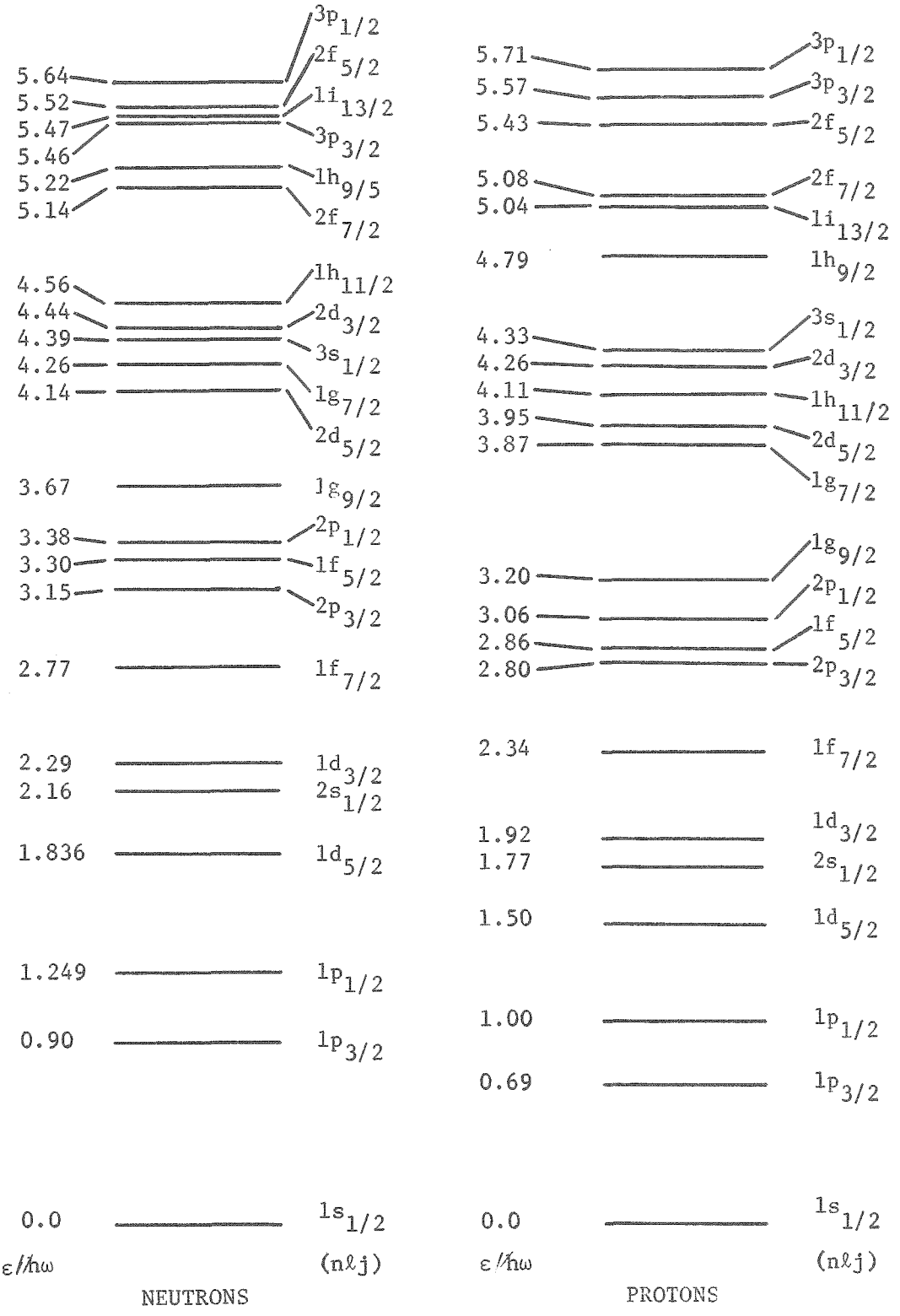

Figure 1. Single Particle Energies for a Woods-Saxon Potential (see text for details).

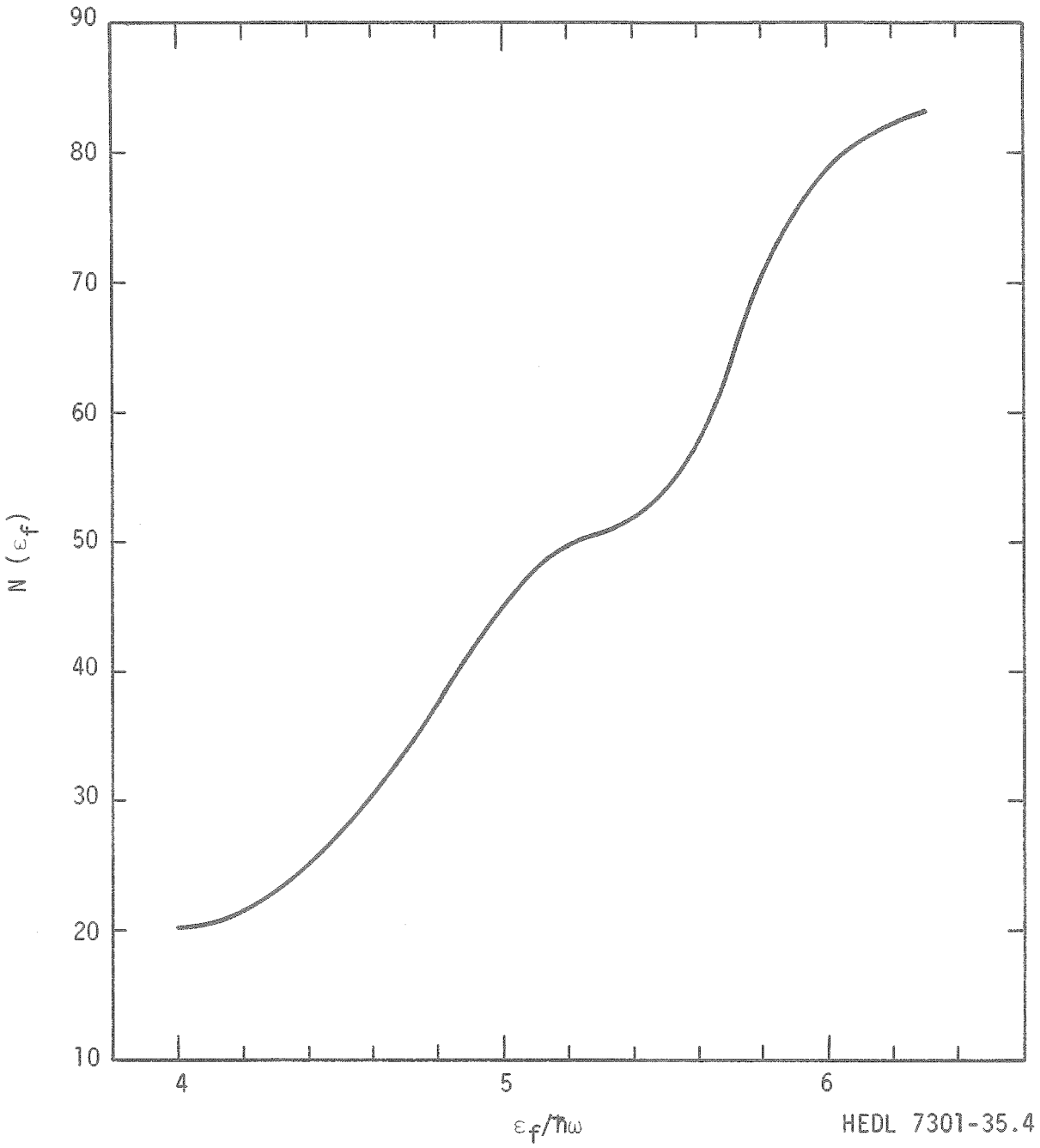

Figure 2. Neutron Occupation Number Versus the Fermi Energy for a Strutinsky-Averaged System (γ = 0.2 $\hbar\omega$).

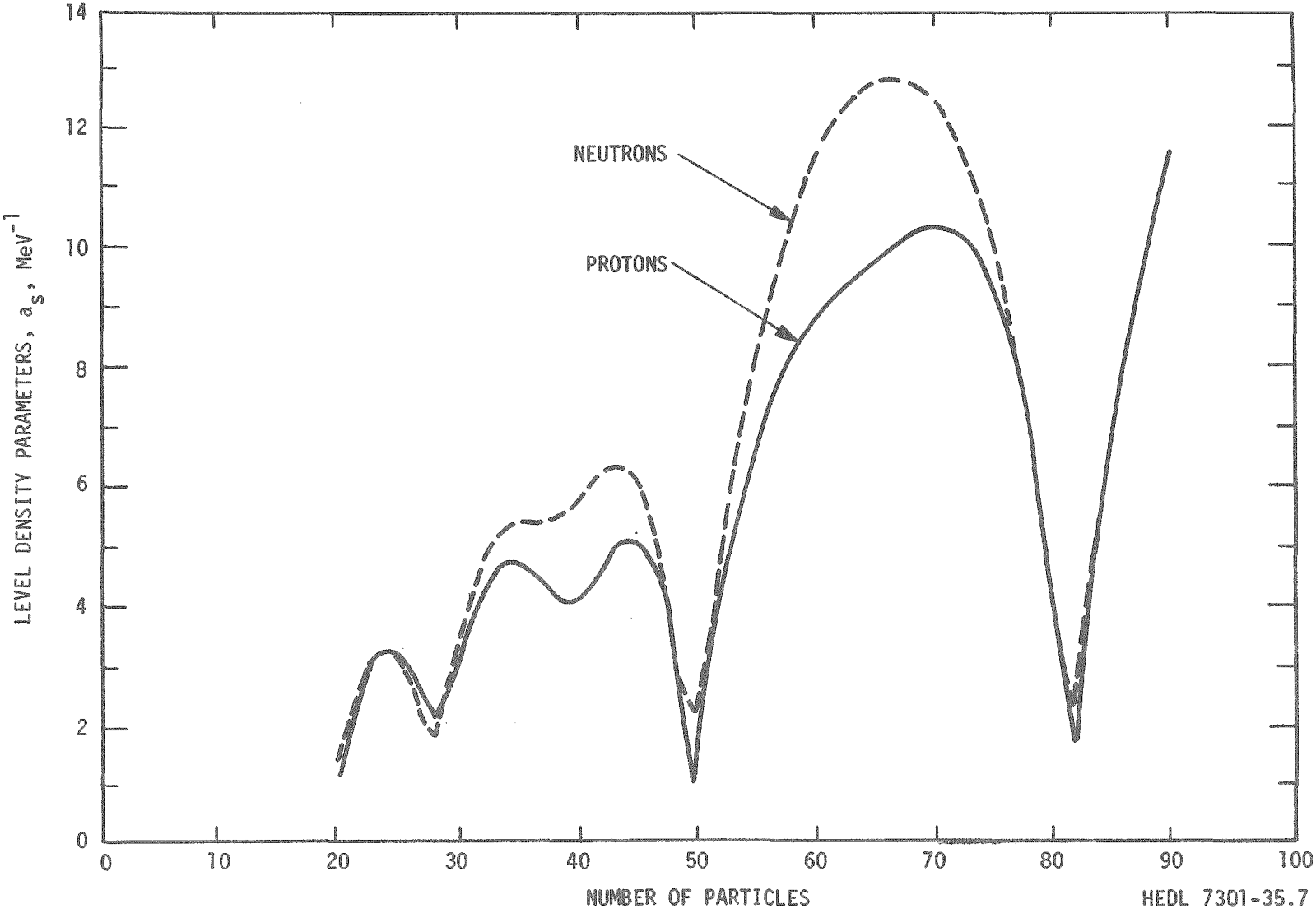

Figure 3. Strutinsky-Averaged Single-Particle Level Densities for Neutrons and Protons.

are essentially the neutron binding energies, $B_n \approx 6$ MeV. With a representative value of 15 MeV^{-1} for the level density parameter a, we find (Eq. (8)) $t \approx .63$ MeV. We have used $\gamma = .2\hbar\omega$ in our calculations, which corresponds to $\gamma = 1.7$ MeV for mass $A \approx 100$. Although this γ is somewhat larger than typical temperatures, we find that a smaller γ does not sufficiently smooth the levels.

The most striking feature of the single-particle level densities is the well-known minima at the magic numbers N - 20, 28, 40, 82, ... Thus, nuclei near-magic numbers have very small level densities. Notice also that in addition to the sharp minima due to shell effects, there is a gradual increase in the level densities with N or Z. This behavior can also be explained by the liquid-drop model of the nucleus.

III. EXPERIMENTAL LEVEL DENSITIES

A. Introduction

In the previous section, we presented theoretical estimates for the single-particle level densities g_s which in turn may be used to compute compound-nucleus level densities, and finally, the observed s-wave resonance spacing D_{obs}. In this section we examine experimental values of D_{obs}. As explained earlier, these values are needed to test and to refine our theoretical estimates.

In spite of recent evaluations there are important discrepancies for many isotopes as seen in Table I, where we compare our results with those of other evaluations. Some of the differences are due to different methods.

Table I

Experimental and Theoretical Values for the

s-wave Resonance Spacing, D_{obs}

Target Nucleus	Benzi[a]	Musgrove[b]	Baba[c]	Exp.	Theory	Ref.
$_{29}Cu^{63}$	1216	813	1060	836 ± 107	553	10
$_{29}Cu^{65}$	1308	1150	1170	1337 ± 284	1502	10
$_{30}Zn^{64}$	4300	2450	3400	3818 ± 1230	2071	11
$_{30}Zn^{66}$	6000	4200	5600	3251 ± 869	6340	11
$_{30}Zn^{67}$	523	671	720	605 ± 258	350	11
$_{31}Ga^{69}$	336	232	320	323 ± 109	159	11
$_{31}Ga^{71}$	352	252	190	140 ± 70.9	214	11
$_{32}Ge^{70}$	3542	1690	2000	1389 ± 248	1684	12
$_{32}Ge^{72}$	3790	1230	3900	1787 ± 499	1674	12
$_{32}Ge^{73}$	96	124	77	74.8 ± 10.8	82.2	12
$_{32}Ge^{74}$	5304	3030	8500	4987 ± 1180	3349	12
$_{32}Ge^{76}$	3489	6270	8000	5430 ± 1490	6738	12
$_{33}As^{75}$	74	60.3	87.3	75.4 ± 16.3	67.4	11
$_{34}Se^{74}$	1628	629	200	353 ± 97.5	329	13
$_{34}Se^{76}$	1237	1950	1200	954 ± 182	944	13
$_{34}Se^{77}$	100	140	150	89.8 ± 11.5	97.6	13
$_{34}Se^{78}$	1141	2650	4500	2540 ± 300	1875	13
$_{34}Se^{80}$	5598	3110	1600	2902 ± 1650	4632	13
$_{34}Se^{82}$	2927	15300	6900	9136 ± 2300	38300	13
$_{35}Br^{79}$	45.2	48.4	61	63.1 ± 17.5	45.9	11
$_{35}Br^{81}$	90	56.3	52	103 ± 54.4	129	11
$_{37}Rb^{85}$	127	72.7	1100	308 ± 186	272	11
$_{37}Rb^{87}$	1319	1220	1800	503 ± 390	2150	11
$_{38}Sr^{84}$	425	367	350	440 ± 109	672	11
$_{38}Sr^{86}$	2167	2470	2100	1975 ± 962	3827	11
$_{38}Sr^{87}$	308	301	210	324 ± 87.2	345	11
$_{38}Sr^{88}$	7000	21100	12000	47010 ± 19400	18270	11
$_{39}Y^{89}$	2505	1990	1600	3478 ± 779	1745	11
$_{40}Zr^{90}$	6254	6850	3300	5282 ± 995	6572	14
$_{40}Zr^{91}$	572	646	250	507 ± 111	317	15

Table I (continued)

Target Nucleus	Benzi	Musgrove	Baba	Exp.	Theory	Ref.
$_{40}Zr^{92}$	3286	2890	3400	2300 ± 775	3178	15
$_{40}Zr^{94}$	3982	3410	3300	5689 ± 3130	2018	15
$_{40}Zr^{96}$	4117	2930	1100	1136 ± 324	1609	11
$_{41}Nb^{93}$	87	122	36.0	89.7 ± 16.0	101	11
$_{42}Mo^{95}$	95	82.2	100	114 ± 35.2	127	16
$_{42}Mo^{96}$	907	1340	1200	1387 ± 597	1313	16
$_{42}Mo^{97}$	75	91.2	120	77.5 ± 17.7	62.9	16
$_{42}Mo^{98}$	1156	1010	790	1014 ± 112	1021	16
$_{42}Mo^{100}$	1561	1200	400	1339 ± 1040	1253	16
$_{44}Ru^{99}$	28.6	25.0	200	34.6 ± 4.52	36.9	17
$_{44}Ru^{101}$	17	13.8	15	18.3 ± 3.80	11.5	17
$_{44}Ru^{104}$	662	784		285 ± 81.0	679	17
$_{45}Rh^{103}$	33	27.3	10.3	27.4 ± 3.07	27.9	11
$_{46}Pd^{105}$	9.55	12.8	11.1	10.1 ± 1.60	9.62	11
$_{47}Ag^{107}$	21	11.8	50	32.2 ± 8.45	15.5	18
$_{47}Ag^{109}$	19	11.8	19.1	19.5 ± 2.54	20.9	18
$_{48}Cd^{111}$	30	33.9	34	32.4 ± 7.03	28.8	11
$_{48}Cd^{113}$	25.9	22.7	27	25.2 ± 3.65	45.3	11
$_{49}In^{113}$	7.32	5.68	7.1	23.9 ± 5.08	15.0	19
$_{49}In^{115}$	9.14	5.74	9.5	$11.6 \pm .996$	24.0	19
$_{50}Sn^{117}$	57	20.0	65.0	57.2 ± 15.3	88.2	11
$_{50}Sn^{118}$	1051	1100	730	614 ± 192	1250	11
$_{50}Sn^{119}$	77	93.8	62.0	179 ± 25.7	114	11
$_{50}Sn^{120}$	1531	543	240	744 ± 577	1807	11
$_{50}Sn^{122}$	2116	1100		4886 ± 3780	3008	11
$_{51}Sb^{121}$	9.6	12.5	13	13.7 ± 1.65	11.5	11
$_{51}Sb^{123}$	34	27.1	30	23.4 ± 6.03	19.8	11
$_{52}Te^{122}$	195	120	130	132 ± 16.0	102	20
$_{52}Te^{123}$	19	24.0	33	26.3 ± 4.07	13.5	20
$_{52}Te^{124}$	499	293		147 ± 12.5	199	20

Table I (continued)

Target Nucleus	Benzi	Musgrove	Baba	Exp.	Theory	Ref.
$_{52}Te^{125}$	48	54.9	46	37.8 ± 2.75	18.6	20
$_{52}Te^{126}$	741	936		207 ± 20.0	475	20
$_{52}Te^{128}$	2250	1930		263 ± 33.4	1477	20
$_{52}Te^{130}$	6290	5610	5700	872 ± 147	8400	20
$_{53}I^{127}$	13	12.1	19	14.7 ± 2.44	6.31	11
$_{53}I^{129}$		27.1	21	26.1 ± 6.66	21.7	11
$_{54}Xe^{129}$	34	10.9		36.2 ± 10.7	10.7	21
$_{54}Xe^{131}$	34	25.0	31	39.2 ± 7.62	25.0	21
$_{55}Cs^{133}$	22	18.5	20.7	20.2 ± 3.32	18.4	11
$_{55}Cs^{136}$		272		71.7 ± 12.9	258	22
$_{56}Ba^{135}$	45	34.9	35	37.1 ± 9.37	31.0	11
$_{56}Ba^{137}$	214	215	460	522 ± 312	763	11
$_{57}La^{138}$	39	30.0	41	35.7 ± 7.58	38.5	11
$_{57}La^{139}$	484	257	110	312 ± 45.8	362	19
$_{59}Pr^{141}$	114	75.5	83.8	63.9 ± 10.4	68.6	11
$_{60}Nd^{142}$	2340	781		415 ± 53.6	957	20
$_{60}Nd^{143}$	34	27.9	19	32.0 ± 2.39	22.0	20
$_{60}Nd^{144}$	677	225		537 ± 71.3	739	20
$_{60}Nd^{145}$	24.1	24.3	25	18.9 ± 1.10	20.4	20
$_{60}Nd^{146}$	370	184		211 ± 24.9	354	20
$_{60}Nd^{148}$	217	138		72.0 ± 6.86	104	20
$_{62}Sm^{147}$	6.5	3.96	7.9	8.18 ± 1.43	6.44	11
$_{62}Sm^{149}$	3.1	1.67	3.22	$2.88 \pm .345$	.795	11

(a) Ref. 7

(b) Ref. 4

(c) Ref. 5

Musgrove[4], for example, has used neutron-capture results to some extent to provide indirect values of D_{obs}. On the other hand, Baba[5], whose technique is close to ours, relies strongly on data from BNL-325, data which are already outdated for many cases.

B. Data Analysis

To find the average resonance spacing D_{obs} from observed resonances, one often introduces the stair-step function $N_{exp}(E)$ defined as the number of resonances below the energy E. The average spacing may then be found by minimizing the following integral[23]:

$$\Delta = \frac{1}{E_N - E_o} \int_{E_o}^{E_1} \left\{ N_{exp}(\varepsilon) - N(\varepsilon) \right\}^2 \, d\varepsilon \quad , \tag{20}$$

where

$$N(E) = (E - E_p) \; / \; D_{obs} \quad . \tag{21}$$

One can allow both E_p and D_{obs} to vary, although we have set $E_p = E_o = 0$ in most cases. In a few cases, where it was obvious that due to experimental reasons low energy resonances were missed, we fixed E_o at some nonzero value to exclude the region of missed resonances. More frequently, resonances are missed at higher energies. This effect is usually very noticeable in a graph of $N_{exp}(E)$, and for each isotope we have selected E_1 to exclude these high energy regions. Figure 4 shows a typical staircase plot with a fitted

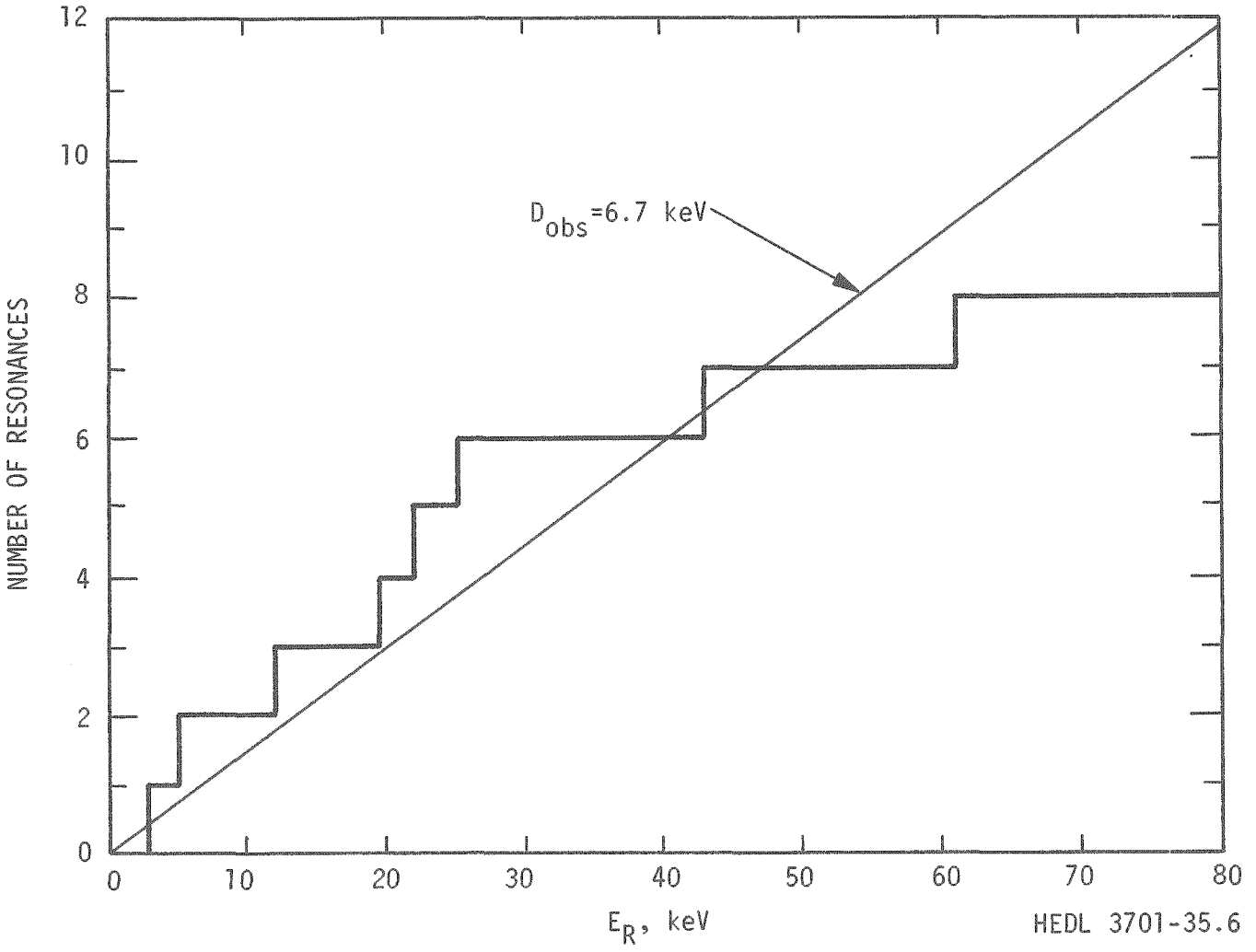

Figure 4. A Stairstep Plot for Ge^{74} with a Preliminary Fit.

straight line N(E). The actual fitting was done by a computer search code called STEPIT.

C. Elimination of p-Wave Resonances

We have defined D_{obs} to be the s-wave resonance spacing, and it is therefore important to eliminate any p-wave resonances that may be counted. Except for isotopes near a maximum in the p-wave strength function, p-wave resonances are so small that they often are completely undetected. Except for those cases where experimenters made specific ℓ-assignments for resonances, we have eliminated p-waves by a method due to Bollinger and Thomas[28]. A probability P_p that a resonance is a p-wave is computed on the basis of its size. Then if P_p is greater than 1/2 it is taken to be a p-wave and is discarded. P_p is computed from

$$P_p\ (g\Gamma_n) = \left\{ 1 + \alpha_I \sqrt{\frac{\langle g\Gamma_{n1} \rangle}{\langle g\Gamma_{no} \rangle}}\ \exp\left[\frac{g\Gamma_n}{2} \left(\frac{1}{\langle g\Gamma_{n1} \rangle} - \frac{1}{\langle g\Gamma_{no} \rangle} \right) \right] \right\}^{-1}, \quad (22)$$

where $g\Gamma_n$ is the usual statistical factor g times the neutron width Γ_n. The average s-wave and p-wave neutron widths may be found from their respective strength functions S_o and S_1 and from the s-wave spacing D_{obs}

$$\langle g\Gamma_{no} \rangle = \sqrt{E}\ D_{obs}\ S_o \quad (23a)$$

$$\langle g\Gamma_{n1} \rangle = \sqrt{E}\ v_1\ (kr)\ D_{obs}\ S_1 \quad . \quad (23b)$$

The penetration factor v_1 (kr) is approximately

$$v_1(kr) \simeq 10^{-7} A^{2/3} E, \text{ eV.} \tag{24}$$

In most cases, fortunately, precise values of S_o, S_1, and D_{obs} are not needed to decide whether or not P_p is larger than 1/2. Rough initial guesses were made for D_{obs} while the strength functions, S_0 and S_1, were obtained by interpolating from known values[14,29,30].

D. Uncertainties

In order to have meaningful experimental values for D_{obs}, we must examine the uncertainties involved. The uncertainties associated with D_{obs} fall into two categories: 1) errors due to poor quality data, and 2) statistical fluctuations of the resonance spacings. Errors of the first type include items like undetected resonances, incorrect identification of s- and p-wave resonances, and resonances associated with the wrong isotope for elements with several naturally-occurring isotopes. Statistical errors become smaller, of course, if a larger number of resonances and hence their spacings, have been measured.

Although we used the more complicated procedure described above to determine D_{obs}, a simple average is easier to analyze for uncertainties. Let E_i denote the energies of N resonances and take D_{obs} to be an average of the N-1 spacings:

$$D_{obs} = \frac{1}{N-1} \sum_{i=1}^{N-1} (E_{i+1} - E_i) \tag{25a}$$

$$= \frac{1}{N-1} \quad (E_N - E_1) \quad . \tag{25b}$$

An unbiased estimate of the variance of the spacings $D_i = (E_{i+1} - E_i)$ is

$$s_D^2 = \frac{1}{N-2} \sum_{i=1}^{N-1} (D_i - D_{obs})^2 \tag{26}$$

where D_{obs} is estimated from Eq. (25). The variance of this estimate for D_{obs} is then given by

$$\sigma_D^2 = \frac{1}{N-1} \quad s_D^2$$

$$= \frac{1}{(N-2)\ (N-1)} \sum_{i=1}^{N-1} (E_{i+1} - E_i - D_{obs})^2 \quad . \tag{27}$$

All of our experimental uncertainties for D_{obs} are given as one standard deviation, $D_{obs} \pm \sigma_D$.

Based on the Wigner distribution of nearest-neighbor spacings, a theoretical estimate of the variance due to statistical fluctuations can be given for spin-zero target nuclei, namely[23]

$$s_D^2 = 0.273\ D_{obs}^2 \quad . \tag{28}$$

We have compared this value with experimental values by computing

$$\left(\frac{s_D}{D_{obs}}\right)^2 = (N-1)\left(\frac{\sigma_D}{D_{obs}}\right)^2 \qquad (29)$$

for about 20 even-even nuclei. The experimental values average to about $(S_D / D_{obs})^2 \approx 0.43$, which indicates that roughly half the variance is due to statistical fluctuations and half is due to the quality of data. Recently, the Columbia group[31] has measured resonances in Eu^{166} to very high accuracy. It is gratifying to note that $(S_D / D_{obs})^2 \approx 0.27$ for the first 25 resonances in agreement with the theoretical value.

The source of data[20] for the Te and Nd isotopes gave evaluated values for D_{obs} along with the number of resonances used rather than individual resonance energies. To estimate errors for these isotopes, we assumed, somewhat arbitrarily, that

$$(S_D / D_{obs})^2 = .6 \quad . \qquad (30)$$

Our evaluated values and uncertainties for D_{obs} are given in Table 1. In the next section we compare these values with theoretical estimates.

IV. COMPARISON OF THEORETICAL AND EXPERIMENTAL LEVEL-DENSITY PARAMETERS

A. Preliminary Comparison

With the aid of the formalism discussed in Section II, we can compare the experimental values for D_{obs} with the theoretical values for the level density parameter a. For each value of D_{obs}, Eqs. (4,7,8 and 10) were

solved for the level density parameter a with the aid of the computer search routine STEPIT. This procedure was carried out for each isotope and defines a set of experimental level-density parameters a_{exp}. We formally represent this relation by

$$a_{exp} = a_{exp}\ (D_{obs}) \quad . \tag{31}$$

By the same means, asymmetrical errors for a_{exp} are defined by

$$a_{exp} \pm \sigma_a^{(\pm)} = a_{exp}\ (D_{obs} \pm \sigma_D) \quad . \tag{32}$$

These experimental level-density parameters are given in Table II along with values for the binding energies B_n and the required pairing energies P. The latter were taken from Gilbert and Cameron's work[3]. Values for the average of the square magnetic quantum number $\langle m^2 \rangle$ needed to compute the spin-cutoff parameter σ (Eq. 7) were obtained from

$$\langle m^2 \rangle \simeq 0.146\ A^{2/3} \quad , \tag{33}$$

a result given by Gilbert and Cameron[3] and derived by Jensen and Luttinger[32]. It has been argued[33] that Eq. (33) should be modified. However, the detailed neglect of the pairing interaction casts doubt on any formula of this type. In any case, the main effect of changing this relation would be to renormalize the a_{exp}. Partly for this reason, small systematic discrepancies of a_{exp} between various evaluations should not be considered signif-

Table II

Values for the Level-Density Parameter a Deduced from Experimental Resonance Spacings, D_{obs}

Target Nucleus	Spin	Bn	Pairing Energies[a]	$a_{exp.}$
29Cu63	3/2	7.9159	0	$8.30^{+.16}_{-.14}$
29Cu65	3/2	7.0604	0	$8.59^{+.30}_{-.23}$
30Zn64	0	7.9881	1.06	$8.94^{+.51}_{-.36}$
30Zn66	0	7.0534	1.06	$10.40^{+.48}_{-.35}$
30Zn67	5/2	10.2024	2.56	$8.76^{+.67}_{-.42}$
31Ga69	3/2	7.6422	0	$9.82^{+.52}_{-.37}$
31Ga71	3/2	6.5197	0	$12.57^{+1.11}_{-.63}$
32Ge70	0	7.4154	1.36	$11.70^{+.31}_{-.26}$
32Ge72	0	6.7853	1.36	$12.48^{+.57}_{-.42}$
32Ge73	9/2	10.1969	3.24	$12.52^{+.23}_{-.19}$
32Ge74	0	6.4859	1.36	$11.34^{+.47}_{-.36}$
32Ge76	0	6.0321	1.36	$12.16^{+.60}_{-.45}$
33As75	3/2	7.3262	0	$12.29^{+.35}_{-.28}$
34Se74	0	8.0255	1.43	$13.02^{+.51}_{-.38}$
34Se76	0	7.4154	1.43	$12.55^{+.35}_{-.28}$
34Se77	1/2	10.4909	2.90	$12.54^{+.20}_{-.17}$
34Se78	0	6.9717	1.43	$11.79^{+.21}_{-.18}$
34Se80	0	6.7144	1.43	$12.09^{+1.49}_{-.76}$
34Se82	0	5.9900	1.43	$11.57^{+.54}_{-.41}$

Table II (continued)

Target Nucleus	Spin	Bn	Pairing Energies[(a)]	$a_{exp.}$
35Br79	3/2	7.8789	0	$11.83^{+.44}_{-.33}$
35Br81	3/2	7.5964	0	$11.56^{+1.04}_{-.57}$
37Rb85	5/2	8.6374	0	$8.81^{+1.07}_{-.52}$
37Rb87	3/2	6.1306	0	$11.52^{+2.40}_{-.87}$
38Sr84	0	8.4824	1.24	$11.85^{+.41}_{-.32}$
38Sr86	0	8.4372	1.24	$9.87^{+.90}_{-.52}$
38Sr87	9/2	11.1005	2.17	$8.52^{+.33}_{-.24}$
38Sr88	0	6.3924	1.24	$8.00^{+.80}_{-.50}$
39Y89	1/2	6.8691	0	$8.67^{+.33}_{-.25}$
40Zr90	0	7.1940	1.20	$10.12^{+.31}_{-.25}$
40Zr91	5/2	8.6403	1.92	$10.34^{+.35}_{-.27}$
40Zr92	0	6.7497	1.20	$12.21^{+.70}_{-.49}$
40Zr94	0	6.4675	1.20	$11.25^{+1.37}_{-.73}$
40Zr96	0	5.5756	1.20	$16.56^{+.74}_{-.55}$
41Nb93	9/2	7.2139	0	$12.03^{+.28}_{-.22}$
42Mo95	5/2	9.1567	2.40	$12.49^{+.55}_{-.40}$
42Mo96	0	6.8161	1.28	$13.17^{+1.00}_{-.61}$
42Mo97	5/2	8.6422	2.57	$14.39^{+.45}_{-.34}$
42Mo98	0	5.9187	1.28	$16.04^{+.25}_{-.22}$

Table II (continued)

Target Nucleus	Spin	Bn	Pairing Energies[(a)]	$a_{exp.}$
42Mo100	0	5.3901	1.28	$17.14^{+3.58}_{-1.30}$
44Ru99	5/2	9.6711	2.57	$13.77^{+.21}_{-.19}$
44Ru101	5/2	9.2161	2.22	$14.98^{+.37}_{-.30}$
44Ru104	0	5.9765	1.28	$18.73^{+.76}_{-.55}$
45Rh103	1/2	7.0020	0	$15.81^{+.20}_{-.18}$
46Pd105	5/2	9.5474	2.59	$16.07^{+.29}_{-.24}$
47Ag107	1/2	7.2756	0	$15.08^{+.49}_{-.37}$
47Ag109	1/2	6.8240	0	$16.85^{+.24}_{-.21}$
48Cd111	1/2	9.3996	2.50	$15.86^{+.41}_{-.32}$
48Cd113	1/2	9.0479	2.68	$17.53^{+.29}_{-.28}$
49In113	9/2	7.3114	0	$13.93^{+.36}_{-.28}$
49In115	9/2	6.7244	0	$16.21^{+.15}_{-.14}$
50Sn117	1/2	9.3310	2.34	$14.83^{+.51}_{-.38}$
50Sn118	0	6.4810	1.19	$15.60^{+.73}_{-.51}$
50Sn119	1/2	9.1100	2.43	$13.60^{+.25}_{-.21}$
50Sn120	0	6.1812	1.19	$16.06^{+3.13}_{-1.13}$
50Sn122	0	5.9319	1.19	$13.06^{+2.95}_{-1.07}$
51Sb121	5/2	6.7982	0	$16.10^{+.21}_{-.19}$

Table II (continued)

Target Nucleus	Spin	Bn	Pairing Energies	$a_{exp.}$ [a]
51Sb123	7/2	6.4316	0	$15.78^{+.51}_{-.39}$
52Te122	0	6.9434	1.14	$17.27^{+.25}_{-.22}$
52Te123	1/2	9.4084	2.57	$16.51^{+.29}_{-.24}$
52Te124	0	6.6034	1.14	$18.05^{+.18}_{-.17}$
52Te125	1/2	9.0924	2.23	$15.87^{+.13}_{-.12}$
52Te126	0	6.3134	1.14	$18.25^{+.21}_{-.19}$
52Te128	0	6.1164	1.14	$18.41^{+.29}_{-.26}$
52Te130	0	5.8954	1.14	$16.59^{+.39}_{-.33}$
53I127	5/2	6.7971	0	$16.06^{+.31}_{-.26}$
53I129	7/2	6.4984	0	$15.52^{+.50}_{-.38}$
54Xe129	1/2	9.2594	2.32	$15.84^{+.59}_{-.43}$
54Xe131	3/2	8.9323	2.16	$15.02^{+.36}_{-.29}$
55Cs133	7/2	6.7044	0	$15.55^{+.30}_{-.25}$
55Cs136	5	8.6114	0.85	$11.88^{+.27}_{-.21}$
56Ba135	3/2	9.2314	2.28	$14.81^{+.47}_{-.36}$
56Ba137	3/2	8.5414	2.43	$12.14^{+1.48}_{-.74}$
57La138	5	8.7894	0.85	$12.58^{+.33}_{-.26}$
57La139	7/2	5.0004	0	$14.68^{+.31}_{-.25}$
59Pr141	5/2	5.8534	0	$15.77^{+.32}_{-.27}$

Table II (continued)

Target Nucleus	Spin	Bn	Pairing Energies[a]	$a_{exp.}$
60Nd142	0	6.1004	1.18	$17.83^{+.29}_{-.26}$
60Nd143	7/2	7.8294	1.94	$16.70^{+.15}_{-.13}$
60Nd144	0	5.7434	1.18	$18.48^{+.33}_{-.28}$
60Nd145	7/2	7.5614	2.10	$18.94^{+.12}_{-.11}$
60Nd146	0	5.2874	1.18	$22.59^{+.33}_{-.29}$
60Nd148	0	5.0414	1.18	$26.81^{+.30}_{-.26}$
60Nd150	0	5.4054	1.18	$23.57^{+.24}_{-.22}$
62Sm147	7/2	8.1424	2.14	$19.01^{+.38}_{-.31}$
62Sm149	7/2	7.9824	2.21	$21.86^{+.27}_{-.24}$

(a) Ref. 3

icant.

The values for a_{exp} are plotted versus the target mass number A in Figure 5 to show their overall behavior. The striking dips at $(A+1) \approx 90$ and 140 may be readily correlated with dips in the theoretical neutron and proton level-density parameters shown in Figure 3, the first dip corresponding to N = 50 and Z = 40, the second corresponding to N = 82. Also, the lowest values in the range A = 110 - 125 are due to indium and tin isotopes which are near the Z = 50 dip in a_Z.

Because the level-density parameter $\underline{a}$ depends on both N and Z (Eq. 5), it is awkward to compare theoretical and experimental values on a plot like Figure 5. Instead, in Figure 6, we plot the differences

$$\Delta a = a_{th} - a_{exp} \tag{34}$$

where a_{th} is the theoretical value. Straight lines are used to connect all the isotopes for each element. In view of the fact that no parameters have been adjusted, the agreement is good; that is, Δa is small. Nevertheless, in addition to fluctuations of about $\pm$ 1 MeV^{-1}, the theory is systematically low ($\Delta a < 0$), especially near $A \approx 115$. Because of approximations, such as the neglect of residual interactions, and problems, such as the difficulty in estimating the spin-cutoff parameter, these systematic discrepancies are not surprising.

B. Adjustment of Theoretical Values

In order to provide the best estimates of D_{obs}, minor adjustments of

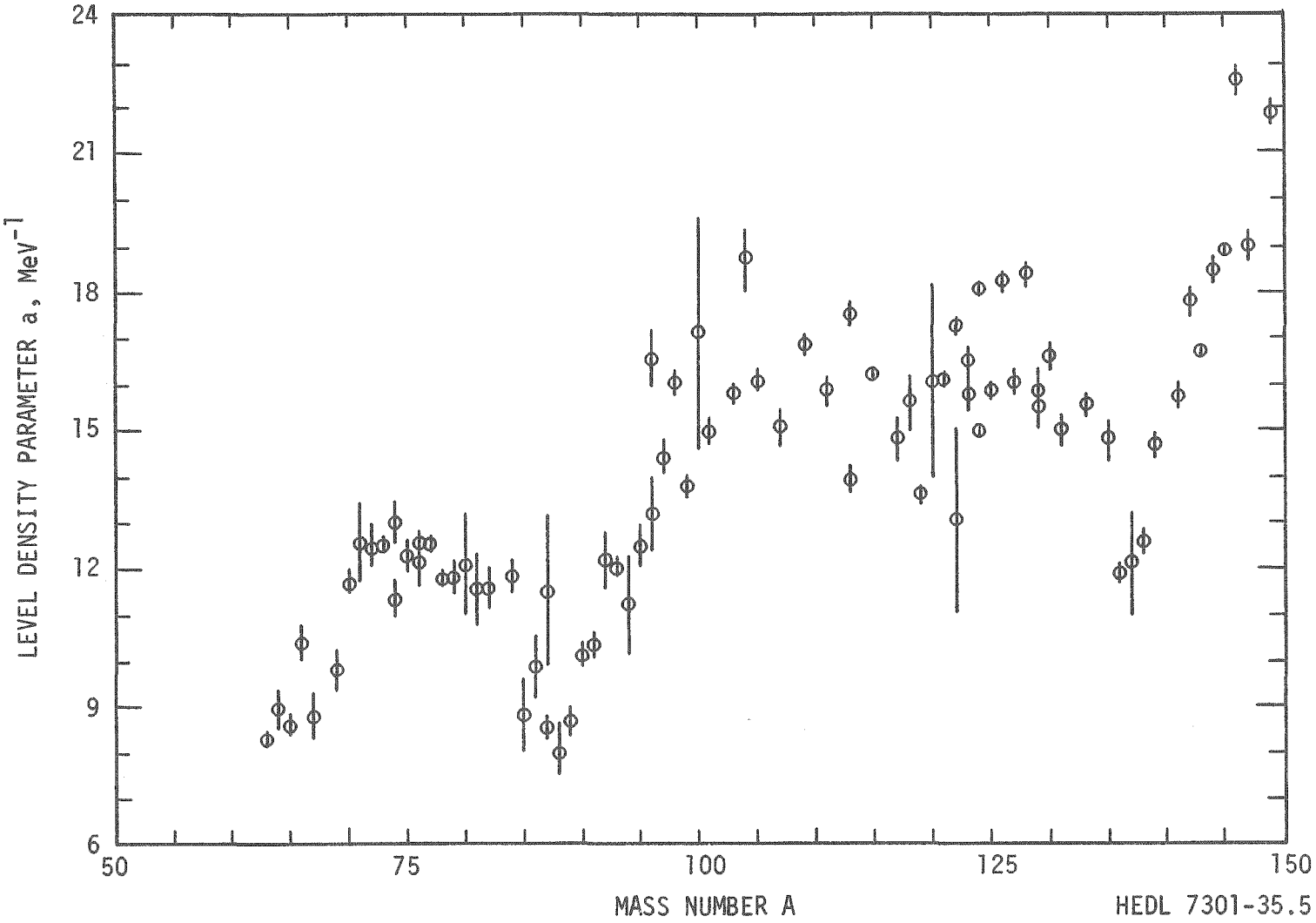

Figure 5. Experimental Level Density Parameters, a_{exp}.

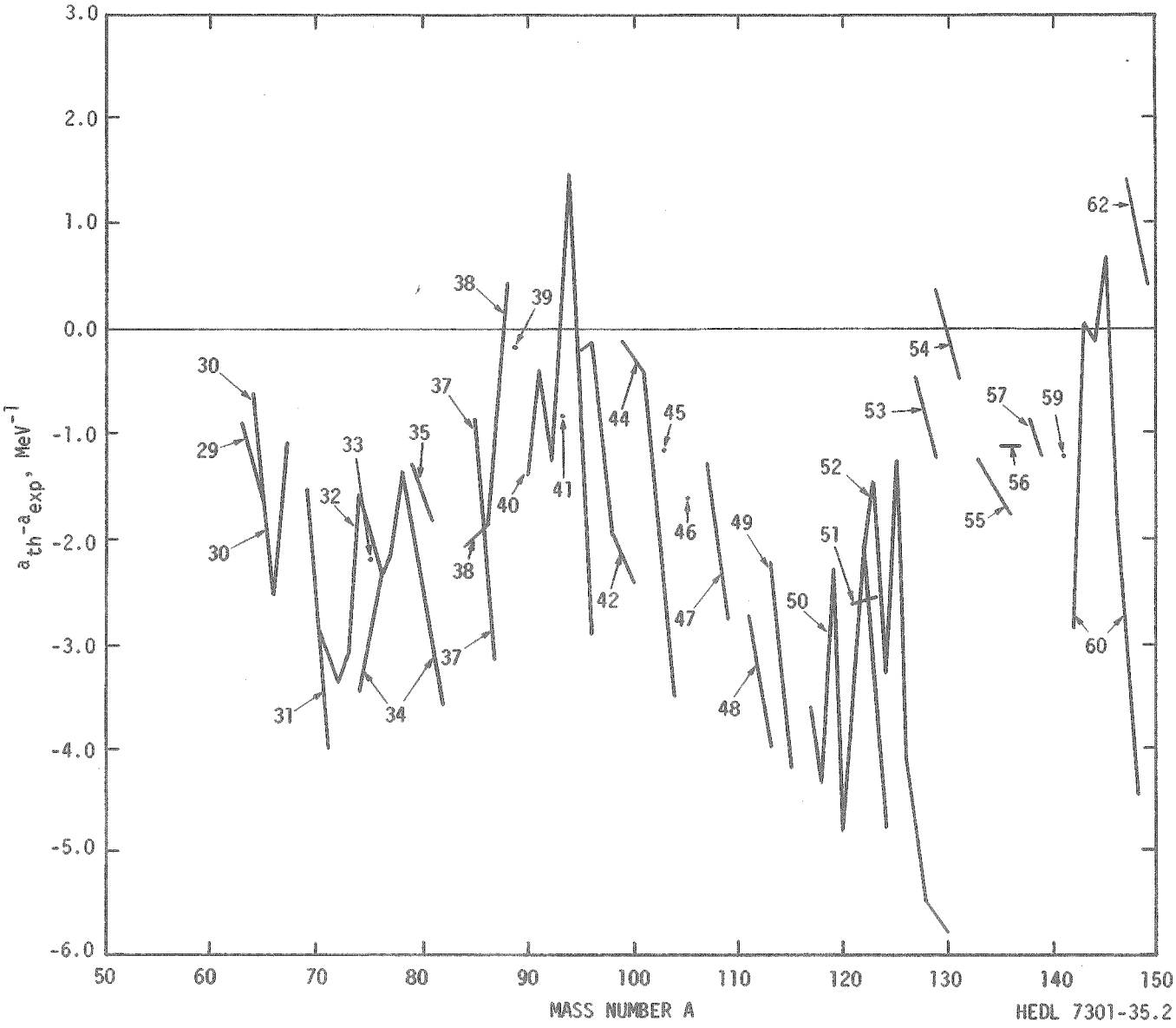

Figure 6. Differences Between Theoretical and Experimental Values for the Level Density Parameter a.

the theoretical estimates for a_N and a_Z were made with the computer program STEPIT by minimizing the function

$$\chi^2 = \frac{1}{N} \sum_{i=1}^{N} \left[\frac{a_{th}(i) - a_{exp}(i)}{\sigma_i^2} \right]^2 \quad . \tag{35}$$

The sum is over all isotopes for which we obtained an experimental value a_{exp} with standard deviation σ_i. The adjusted theoretical value for the i-th isotope is given by

$$a_{th}(i) = F_N(N)\, a_N(N) + F_Z(Z)\, a_Z(Z) \quad , \tag{36}$$

where the adjustment functions F_N and F_Z are smooth functions near the value 1 for all N and Z. Several functional forms for the F's were tried. The following form worked as well as any:

$$F_s(i) = C_{os} \prod_{k=1}^{3} \left[1 + C_{ks} \exp\left(\frac{i - M_{ks}}{G_{ks}} \right)^2 \right] \quad , \tag{37}$$

where s designates neutrons or protons and i is the respective number of neutrons N or protons Z. The 20 constants C_{os}, C_{ks}, M_{ks}, and G_{ks} were adjusted to minimize χ^2 determined by Eq. (35). Actually, to prevent very local adjustments to a_{th}, the G_{ks} were set equal to 2 even though smaller values gave a slightly better fit.

These final values, given in Table III and used with Eqs. (36) and

Table III

Parameters for Adjusting the Theoretical Level Density Parameter, a_{th}

	Neutrons	Protons		Neutrons	Protons		Neutrons	Protons
C_0	1.29	1.04						
C_1	0.351	0.053	M_1	40.5	32.9	G_1	2.0	2.0
C_2	-.223	-.244	M_2	54.3	44.8	G_2	2.0	2.0
C_3	-.366	-.163	M_3	85.6	53.3	G_3	2.0	2.0

(37), represent our best prescription for estimating the level density parameter $\underline{a}$. The differences between these adjusted values and the experimental values are shown in Figure 7. Although it is awkward to display errors on this figure, it is gratifying to note that many of the large discrepancies are correlated with large experimental uncertainties. There are some notable exceptions; for example, the tellurium and neodymium isotopes.

Theoretical estimates for D_{obs} were computed from our adjusted values for the level density parameter $\underline{a}$ and are compared to experimental values in Table I.

C. Error Estimates

In this section we give a quantitative measure of the errors in the theoretical values for D_{obs}. In general, these errors are large enough that the usual description, $D \pm \sigma_D$, appropriate for a normal distribution, is wrong. In the Appendix, the entire problem of assigning asymmetrical errors of the form $D \pm \Delta^{(\pm)}$ is discussed in detail.

Basically, we assume that the variables $x_i = \ln(D_{ti}) - \ln(D_{xi})$ are normally distributed with mean value zero where D_{ti} and D_{xi} represent the theoretical and experimental values of D_{obs} for the i-th isotope, respectively. Because of the fitting procedures used to determine the theoretical level density parameters a_{ti}, the differences, $a_{ti} - a_{xi}$, should be distributed about zero, see Figure 7. It follows that the x_i have a mean value of zero.

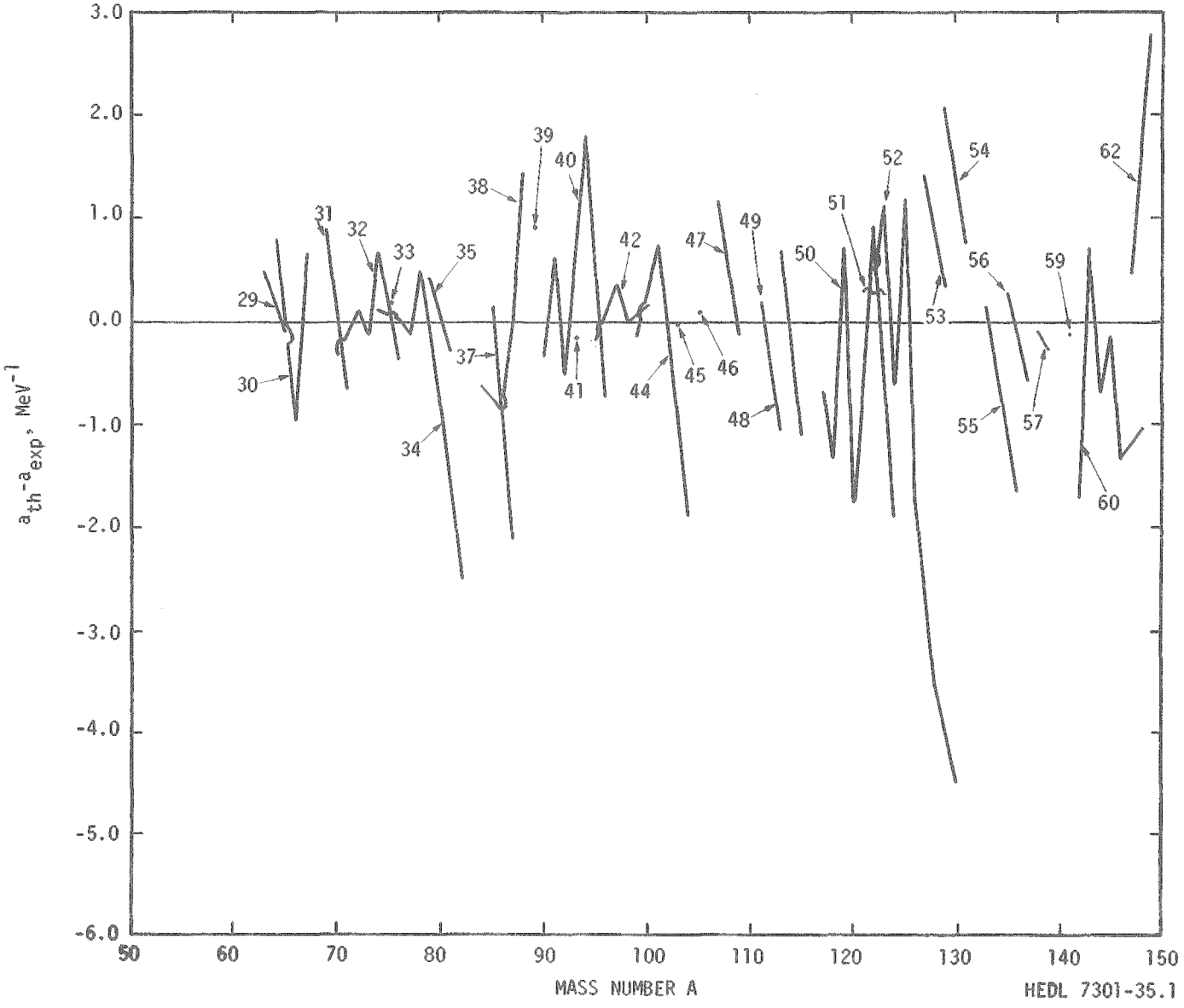

Figure 7. Differences Between Adjusted Theoretical and Experimental Values for the Level Density Parameter a.

An estimate for the variance of the x_i is given by

$$\sigma_x^2 = \frac{1}{N-1} \sum_{i=1}^{N} \left[\ln(D_{ti}) - \ln(D_{xi})\right]^2,$$

where the sum is over all isotopes. Now define a new variable θ_D by

$$\theta_D = e^{\sigma_x}$$

$$= \exp\left\{\left[\frac{1}{N-1} \sum_{i=1}^{N} \ln^2(D_{ti}/D_{xi})\right]^{1/2}\right\}.$$

Since σ_x is the standard deviation for $x_i = \ln(D_{ti}) - \ln(D_{xi})$, θ_D is a corresponding factor for the ratio D_{ti}/D_{xi}. In other words, θ_D is the factor by which the theoretical and experimental level spacings are likely to differ at the usual one-sigma confidence limit.

For the isotopes in this work, we find $\theta_D = 1.87$. For comparison and using the prescription of Gilbert and Cameron[3], we recalculated the $\{D_{ti}\}$ for all the isotopes. These values of $\{D_{ti}\}$ lead to $\theta_D = 2.31$, a value considerably larger than our own.

V. SUMMARY

Experimental neutron resonance spacings were evaluated for over 80 spherical nuclei ($29 \leq Z \leq 62$). A partly phenomenological and partly theoretical prescription was used to estimate these spacings to within a factor

of $\theta_D \approx 1.9$. This factor compares to a value of $\theta_D \approx 2.3$ obtained for these same nuclei with the older formula of Gilbert and Cameron[3].

Finally, we wish to point out that there are exceptions to our assumption that all the nuclei in the region studied are spherical. Xe^{124} is deformed, for example. The parameter adjustments probably overcome this difficulty to some extent. Nevertheless, any results obtained for deformed nuclei in this region should be used with extra caution.

References

1. F. A. Schmittroth, Theoretical Calculations of Fast Neutron Capture Cross Sections, HEDL-TME 71-106, (Hanford Engineering Development Laboratory, August 1971).
2. T. D. Newton, Can. J. Phys. 34 (1956) 804.
3. A. Gilbert and A. G. W. Cameron, Can. J. Phys. 43 (1965) 1446.
4. A. R. de L. Musgrove, Interpolative Formulae for Average Nuclear Level Spacing and Total Radiation Width, AAEC/E211, (Australian Atomic Energy Commission, Lucas Heights, (November 1970).
5. H. Baba and S. Baba, Average Level Spacings and the Nuclear Level Density Parameter, JAERI-1183, (Japan Atomic Energy Research Institute, August 1969).
6. H. Baba, Nuc. Phys. A159 (1970) 625.
7. V. Benzi, et al, Fast Neutron Radiative Capture Cross Sections of Stable Nuclei with $29 \leq Z \leq 79$, Doc. CEC (71) 9, (Bologna, Italy, November 1971).
8. V. M. Strutinski, Sov. J. Nuc. Phys. 3 (1966) 449.
9. V. M. Strutinski, Nuc. Phys. A122 (1968) 1.
10. R. N. Alves, et al, Nucl. Phys. A134 (1969) 118.
11. Murray D. Goldberg, et al, Neutron Cross Sections, BNL-325 Second Edition, Supplement No. 2 (1966).
12. Kh. Maletski, et al, Soviet Atomic Energy 24 (1968) 207.
13. H. Malecki, et al, Soviet J. Nuc. Phys. 9 (1969) 655.
14. J. Morgenstern, et al, Nuc. Phys. A123 (1969) 561.
15. Z. M. Bartolome, et al, Nuc. Sci. and Eng. 37 (1969) 137.

References (cont'd.)

16. H. Weigmann, et al, Proc. 3rd Conf. on Neutron Cross Sections and Technology, (March 15-17, 1971) 749.

17. H. G. Priesmeyer and H. H. Jung, Proc. 3rd Conf. on Neutron Cross Sections and Technology, (March 15-17, 1971) 688.

18. Muradyan, et al, Nuclear Data for Reactors (Proc. Conf. Paris 1966) 1 (October 1966) 79.

19. George Hacken, Ph.D. Thesis, Columbia Univ. (1971).

20. H. Tellier and C. M. Newstead, Proc. 3rd Conf. on Neutron Cross Sections and Technology, (March 15-17, 1971) 680.

21. R. Ribon, et al, Nuclear Data for Reactors (Proc. Conf. Paris 1966) 1 (October 1966) 119.

22. V. P. Vertebny, et al, Nuc. Phys. Research in the USSR (Collected Abstracts) No. 10, INDC(CCP)-15/U (December 1971).

23. J. E. Lynn, The Theory of Neutron Resonance Reactions, Chapter IV, (Clarendon Press, Oxford, 1968).

24. Claude Block, Phys. Rev. 93 (1954) 1094.

25. N. Rosenzweig, Phys. Rev. 108 (1957) 817.

26. L. G. Moretto, Nucl. Phys. A182 (1972) 641.

27. Aage Bohr and Ben R. Mottleson, Nuclear Structure, Vol. I (W. A. Benjamin, Inc., 1969, New York) 238.

28. L. M. Bollinger and G. E. Thomas, Phys. Rev. 171 (1968) 1293.

29. Kamal K. Seth, Nuclear Data, Section A, Vol. 2 (Sept. 1966) 299.

30. D. Kompe, Nuc. Phys. A133 (1969) 513.

31. H. I. Liou, Phys. Rev. C5 (1972) 974.

References (cont'd.)

32. J. H. D. Jensen and J. M. Luttinger, Phys. Rev. 86 (1952) 907.

33. U. Facchini and E. Saetta-Menichella, Ener. Nucleare 15 (1963) 54.

APPENDIX A

Statistical Variables of the Form exp (αa)

A. Introduction

Many statistical parameters associated with neutron cross sections are always positive. Unless the variance of these parameters is small so that the confidence limits associated with normal distributions are appropriate, it is not obvious how to express confidence limits. Suppose, for example, that the average resonance spacing D is expressed as

$$D = D_o \pm \sigma_D \tag{A1}$$

at the one-sigma confidence limit. Since D is always positive, these limits are clearly meaningless for $\sigma_D > D_o$.

The computation of dose rates in reactor shielding provides another example. Roughly speaking, the attenuation of radiation through a shield of thickness x gives a dose rate

$$DR \propto S \exp(-\mu x). \tag{A2}$$

Uncertainties in the dose rate, a quantity which is always positive, arise from uncertainties in both the radiation source strength S and the attenuation factor μ.

An intuitive way to treat a positive variable D is to use logarithms to define a new statistical variable d:

$$d = \ln(D) \quad . \tag{A3}$$

Superficially at least, since d is not restricted to positive values, it makes more sense to apply the statistics of a normal distribution to d than to D. The confidence limits of D may then be expressed in terms of confidence limits for d:

$$D \pm \Delta_D^{(\pm)} = \exp(d \pm \sigma_d). \tag{A4}$$

The $(\pm)$ superscript on $\Delta_D^{(\pm)}$ makes the asymmetrical nature of these limits explicit.

We focus our attention on three problems in the following sections:

1) For what physical quantities are the results appropriate?
2) How are confidence limits for functions of several variables combined?
3) How are these limits most conveniently expressed?

B. Formal Properties

Define a positive statistical variable A by

$$A(a) = C_A \exp(\alpha a), \tag{A5}$$

where C_A ($C_A > 0$) and α are constants, and $\underline{a}$ is another statistical variable.

We now make a key assumption. Assume that the variable $\underline{a}$ is normally

distributed with mean value $\bar{a}$ and variance σ_a^2. This assumption, together with Eq. (A5), completely specifies the statistical properties of A; whether or not A is a good representation for a particular physical variable depends on the particular variable involved.

We have already noted the following property of A:

$$A > 0 \ . \tag{A6}$$

We now find the mean value of A defined by

$$\langle A \rangle = \int_0^\infty A \, f_A \, dA = \int_{-\infty}^\infty A \, f_a \, da \ , \tag{A7}$$

where f_A is the distribution function for A. Since $\underline{a}$ is normally distributed, its distribution function is

$$f_a = \frac{1}{\sqrt{2\pi}\,\sigma_a} \exp\left[-\frac{1}{2}\left(\frac{a-\bar{a}}{\sigma_a}\right)^2\right] \ . \tag{A8}$$

We note in passing:

$$f_A = \frac{da}{dA} \, f_a \ . \tag{A9}$$

By the technique of completing the square, we find

$$\langle A \rangle = \frac{C_A}{\sqrt{2\pi}\,\sigma_a} \int \exp(\alpha a)\, \exp\left[-\frac{1}{2}\left(\frac{a-\bar{a}}{\sigma_a}\right)^2 \right] da,$$

$$= \frac{A(\bar{a})}{\sqrt{2\pi}\,\sigma_a} \int \exp(\alpha a)\, \exp\left[-\frac{1}{2}\left(\frac{a}{\sigma_a}\right)^2 \right] da,$$

$$= A(\bar{a}) \exp\left[\frac{1}{2}\left(\alpha\sigma_a\right)^2 \right] . \qquad \text{(A10)}$$

The most probable value of A (denoted by A_p) is given by

$$\left. \frac{df_A}{dA} \right|_{A = A_p} = 0 \quad . \qquad \text{(A11)}$$

It is straightforward to show

$$A_p = A(\bar{a} - \alpha\sigma_a^2) \quad ,$$

$$= A(\bar{a}) \exp\left[-(\alpha\sigma_a)^2 \right] . \qquad \text{(A12)}$$

A general picture (Figure A1) of the distribution function, f_A, for A may be formed by noting

$$A_p < A(\bar{a}) < \langle A \rangle \, , \qquad \text{(A13)}$$

and that (see Eqs. A8 and A9)

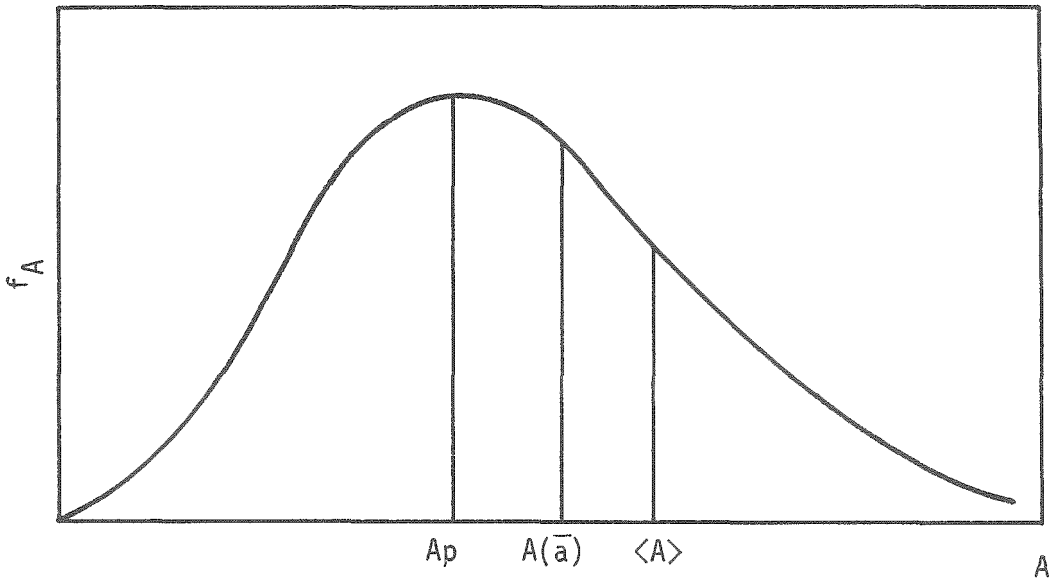

Figure A1. The Distribution Function f_A.

$$f_A = 0 \tag{A14}$$

for $A = 0$ and $A = \infty$.

Next, we find the variance σ_A^2 for A:

$$\sigma_A^2 = \langle A^2 \rangle - \langle A \rangle^2 \quad . \tag{A15}$$

The calculation for $\langle A^2 \rangle$ is similar to that for $\langle A \rangle$, and we obtain

$$\langle A^2 \rangle = A^2(\bar{a}) \cdot \exp\left[2(\alpha\sigma_a)^2\right], \tag{A16}$$

to find

$$\sigma_A^2 = \left\{ \exp\left[(\alpha\sigma_a)^2\right] - 1 \right\} \langle A \rangle^2 . \tag{A17}$$

C. Confidence Limits

A main purpose here is to find a convenient representation for the confidence limits of A. We start from the fact that the one-sigma confidence limits for $\underline{a}$ are given by

$$\bar{a} - \sigma_a \quad < \quad a \quad < \quad \bar{a} + \sigma_a \, . \tag{A18}$$

Since an element of probability may be expressed as

$$dp = f_a \, da = f_A \, dA \quad , \tag{A19}$$

both the left and right-hand sides of the following equation represent the

same fraction of the total probability:

$$\int_{\bar{a}-\sigma_a}^{\bar{a}+\sigma_\alpha} f_a \, da = \int_{A(\bar{a}-\sigma_a)}^{A(\bar{a}+\sigma_a)} f_A \, dA \quad . \tag{A20}$$

Therefore, the following confidence limits for A represent precisely the same limits as those given by Eq. (A18):

$$A(\bar{a}-\sigma_a) < A < A(\bar{a}+\sigma_a) \quad . \tag{A21}$$

A convenient way to express these results is by

$$\frac{A(\bar{a})}{\theta_A} < A < \theta_A \, A(\bar{a}) \quad . \tag{A22}$$

where

$$\theta_A = \exp(\alpha\sigma_a) \quad . \tag{A23}$$

In other words, A is given by $A(\bar{a})$ to within a factor of θ_A at the same confidence level for which $\underline{a}$ is given by $\bar{a} \pm \sigma_a$.

To make these ideas more useful, we want to relate θ_A directly to the variance σ_A^2. In this way, one does not have to seek an underlying variable $\underline{a}$.

First, we combine Eqs. (A10) and (A17) to find

$$\sigma_A^2 = \left\{ \exp\left[(\alpha\sigma_a)^2\right] - 1 \right\} \exp\left[(\alpha\sigma_a)^2\right] A^2(\bar{a}) \quad . \tag{A24}$$

In principle, given σ_A / $A(\bar{a})$, one can compute $(\alpha\sigma_a)$ and hence θ_A. Instead, we define a variable, R, by

$$\sigma_A = R\, A(\bar{a})\, (\theta_A - 1) \quad . \tag{A25}$$

Numerical calculations show that the value of R satisfies

$$.92 < R < 1.1 \tag{A26}$$

for

$$1 < \theta_A < 2.5 \quad . \tag{A27}$$

To within 10%, $R \simeq 1$ for all values of θ_A likely to be encountered. In any real case, this error will likely be unimportant so that

$$\sigma_A \simeq A(\bar{a})\, (\theta_A - 1) \quad . \tag{A28}$$

Given the variance σ_A, one can find confidence limits from

$$\theta_A \simeq 1 + \frac{\sigma_A}{A(\bar{a})} \quad . \tag{A29}$$

The confidence limits, as expressed by the Inequality (A22), may be rewritten as

$$A(\bar{a}) - \Delta_A^{(-)} < A < A(\bar{a}) + \Delta_A^{(+)}, \tag{A30}$$

where

$$\Delta_A^{(+)} = \sigma_A \ , \tag{A31a}$$

and

$$\Delta_A^{(-)} = \left(\frac{1}{1+\sigma_A/A(\bar{a})} \right) \sigma_A \ , \tag{A31b}$$

D. Uncertainties For More Than One Variable

In this section, we discuss how to find uncertainties in (A + B) and (A x B) where A and B are two independent variables of the type considered here.

First consider products:

$$P = A \times B \ . \tag{A32}$$

With notation similar to the previous sections, we have

$$P = C_A \exp\left[\alpha a\right] \times C_B \exp\left[\beta b\right]$$

$$= C_A C_B \exp\left[\alpha a+\beta b\right] \quad , \tag{A33}$$

where a and b are normally distributed. This product has the same form as A and B, namely

$$P = C_p \exp(c) \quad , \tag{A34}$$

where $c = \alpha a+\beta b$. If a and b are normally distributed with variance σ_a^2 and σ_b^2 respectively, c is normally distributed with variance

$$\sigma_c^2 = (\alpha\sigma_a)^2 + (\beta\sigma_b)^2 \quad . \tag{A35}$$

The θ-factor for P is therefore

$$\theta_P = \exp\left\{\left[(\alpha\sigma_a)^2 + (\beta\sigma_b)^2\right]^{\frac{1}{2}}\right\} . \tag{A36}$$

The variance for P may be approximated by Eq. (A28):

$$\sigma_P^2 \simeq P^2(\bar{c}) \ (\theta_p-1)^2 \quad , \tag{A37}$$

where

$$P(\bar{c}) = C_p \exp(\bar{c})$$

$$= C_A C_B \exp(\alpha a + \beta b)$$

$$= A(\bar{a}) \times B(\bar{b}) \quad . \tag{A38}$$

Next consider sums:

$$S = A + B. \tag{A39}$$

We just noted that the product P = A x B has the same exponential form as A and B. However, the sum S does not. Nevertheless, the variance of S is still given by

$$\sigma_S^2 = \sigma_A^2 + \sigma_B^2 \quad , \tag{A42}$$

which is a general property of the variance for independent variables. To the extent for which the exponential form gives a valid approximation for the distribution of S, a θ-Factor θ_S can be obtained from σ_S by Eq. (A29).

E. Use and Summary

For positive statistical variables which may be adequately represented by functions of the form

$$A = C_A \exp(\alpha a) \tag{A43}$$

where $\underline{a}$ is normally distributed, we have shown how to conveniently express confidence limits by the concept of a θ-Factor. In this representation, uncertainties are expressed in terms of a multiplicative factor θ_A, rather than the usual plus and minus notation. We might say, for example, that an experimental neutron flux is known to within a factor of 1.3 as compared to saying it is known to within plus or minus 30%.

As a further illustration of these ideas, we show that our results agree with those given by a normal distribution for small σ_A/A. Thus, variables which are described by a normal distribution do not have to be considered separately if their uncertainties are small.

To the extent that the approximation Eq. (A28) is valid, Eq. (A31) shows that the upper uncertainty $\Delta_A^{(+)}$ is identical to the standard deviation α_A. For a normal distribution, σ_A gives both the upper and lower uncertainties at the one-sigma confidence level. For $1 + \sigma_A/A(\bar{a}) \simeq 1$, Eq. (A31) also shows that the lower uncertainty agrees with the results of a normal distribution: $\Delta_A^{(-)} \simeq \sigma_A$. Finally, from the properties discussed in Section B, it can be shown that the mean value and most probable value coincide, $\langle A \rangle \approx A_p$, for $\sigma_A/A(\bar{a})$ small.

So far, only distributions defined by $A = C_A \exp(\alpha a)$ have been considered. Our results can be extended to the more general form

$$A = C_A \exp[f(a)] \tag{A44}$$

if $f(a)$ may be approximated by a Taylor expansion. It is straightforward

to show that the variance of f is given by

$$\sigma_f^2 = \langle f^2 \rangle - \langle f \rangle^2 \quad , \tag{A45}$$

$$= \left(\frac{df}{da} \right)^2 \sigma_a^2 + (\text{higher order terms}), \tag{A46}$$

where the variance of $\underline{a}$ is

$$\sigma_a^2 = \langle a^2 \rangle - \langle a \rangle^2 \quad . \tag{A47}$$

Hence, the θ-Factor becomes

$$\theta_A = \exp \left[\sqrt{V_f} \right] = \exp \left[\left| \frac{df}{da} \right| \sigma_a \right] . \tag{A48}$$

As an example of this last result, consider an approximate form for the average resonance spacing D:

$$D = C \exp \left[-2 \sqrt{aU} \right] \quad . \tag{A49}$$

Since we have

$$f(a) = -2 \sqrt{aU} \quad , \tag{A50}$$

then

$$\theta_D = \exp \left[\sigma_a \sqrt{U/a} \right] \quad . \tag{A51}$$

DISTRIBUTION

External

No. of Copies	
178	UC-79 Basic List
18	UC-79d Physics
125	Brookhaven National Laboratory

Internal

No. of Copies	
3	AEC, Richland Operations Office
	J.M. Shivley
	T.A. Nemzek
	R.M. Poteat
1	RDT Site Office
	F.R. Standerfer
46	Westinghouse Hanford Company
	R.A. Bennett
	W.L. Bunch
	E.A. Evans
	J.M. Grace
	P.L. Hofmann
	H.T. Knight
	W.W. Little
	R.E. Schenter (15)
	F. Schmittroth (15)
	A. Squire
	S.A. Weber
	Document Control (5)
	Technical Communications (2)